On the Velocity Distribution over the Surface of a Symmetrical Aerofoil at High Speeds. II[1]

Saburô Asaka (阿阪三郎)

Department of Physics, Faculty of Science,
Ochanomizu University, Tokyo

§ 1. Introduction

In the previous paper[(1)] (Part I of this paper) we have presented the general procedures of Imai's thin-wing-expansion method with some modifications and extentions. The usefulness of this method has been demonstrated in several cases, as described in the previous paper. The flow at subsonic speeds past an aerofoil with finite edge angles, which is important from both theoretical and practical points of view, has not yet been studied analytically in detail. In this paper we shall apply the thin-wing-expansion method to a symmetrical biconvex circular arc aerofoil, as a representative of such aerofoils.

§ 2. Procedures of the Calculation

For convenience' sake we shall summarize here the actual procedures for the calculation of the velocity distribution over the surface of an aerofoil.

We consider a symmetrical aerofoil with its chord placed parallel to the undisturbed flow. Let its contour be given by an equation

$$y_p = y_p(x_p) \qquad (-1 \leqq x_p \leqq 1) .$$

This equation is also written using a parameter ϑ in the following form:

$$\left.\begin{aligned} x_p &= \cos\vartheta \qquad (-\pi \leqq \vartheta \leqq \pi) , \\ y_p &= g(\vartheta) = g_1(\vartheta) + g_2(\vartheta) + g_3(\vartheta) + O(\varepsilon^4) . \end{aligned}\right\} \qquad \text{I-(4.10)}^{2)}$$

The points at $\vartheta = 0$ and $\vartheta = \pi$ (or $-\pi$) correspond to the trailing and leading edges of the profile respectively. $g_1(\vartheta)$, $g_2(\vartheta)$ and $g_3(\vartheta)$ are terms of the order of magnitude of ε, ε^2 and ε^3 respectively, ε being a small parameter representing the thickness of the aerofoil.

We consider an auxiliary aerofoil, which is given by the equation in the ζ-plane,

$$\zeta = \xi + i\eta ; \qquad \xi = x , \qquad \eta = \mu y ,$$

---

1) Contribution from Department of Physics, Faculty of Science, Ochanomizu University, No. 21.

2) The equation (4.10) of Part I. Hereafter we shall refer to the equations of the previous paper by this notation.

where $\mu=\sqrt{1-M^2}$, and M is the Mach number of the undisturbed flow. We must first determine the function, by which the region outside the profile in the ζ-plane is mapped onto the region outside the unit circle in the Z-plane ($Z=e^{i\theta}$). If the thickness of the profile is small, this mapping function can be expanded as follows:

$$\left.\begin{aligned}\xi(\theta)&=\cos\theta+\xi_1(\theta)+\xi_2(\theta)+\xi_3(\theta)+O(\varepsilon^4)\,,\\ \eta(\theta)&=\qquad\quad\ \eta_1(\theta)+\eta_2(\theta)+\eta_3(\theta)+O(\varepsilon^4)\,.\end{aligned}\right\}\qquad \text{I–(4.2)}$$

The expressions for $\xi_m(\theta)$ and $\eta_m(\theta)$ in terms of $g_m(\theta)$ ($m=1, 2, 3$) are given by the equations I–(4.13).

The velocity potential is also expanded as follows:

$$\Phi=x+\phi_1+\phi_2+\phi_3+O(\varepsilon^4)\,,\qquad \text{I–(2.5)}$$

where the velocity of the undisturbed flow is assumed to be unity and ϕ_m is the real part of the complex function G_m. The functions G_m are the solutions of the differential equations derived by linearization and iteration, and should obey the following conditions:

(i) $\partial G_m/\partial\zeta$ is one-valued and continuous everywhere in the flow;
(ii) as $\zeta\to\infty$, $\partial G_m/\partial\zeta\to 0$; and
(iii) on the surface of the profile,

$$\Im\left(\frac{\zeta_m}{\mu^2}+G_m\right)=0\,.$$

The full expressions for G_m have been obtained in § 3 of the previous paper: G_1 in I–(3.3), G_2 in I–(3.4) and I–(3.5), and G_3 in I–(3.7) and I–(3.8).

The potential functions ϕ_m have thus been determined successively, so that the velocity distribution over the surface of the aerofoil can be calculated by one of the formulae I–(5.1), I–(5.3), I–(5.5), I–(5.7) and I–(5.8).

The Flow past a Symmetrical Circular Arc Aerofoil

§ 3. The Shape of the Profile and its Mapping Function

The shape of the profile under consideration is shown in Fig. 1. The upper surface of the profile is expressed by the equation,

$$x_p^2+(y_p+\cot 2\beta)^2=\operatorname{cosec}^2 2\beta \qquad (-1\leqq x_p\leqq 1)\,,$$

where 4β denotes the leading or the trailing edge angle. Since the profile is assumed to be sufficiently thin, β is a small quantity and y_p can be expanded in a series of β as follows:

$$y_p=\frac{\beta}{2}(1-\cos 2\vartheta)+\frac{\beta^3}{24}(7-4\cos 2\vartheta-3\cos 4\vartheta)+O(\beta^5)\,.$$

If we use the thickness ratio $t=\tan\beta$ instead of β, the whole contour of the profile is expressed by the equations:

$$\left.\begin{aligned} x_p&=\cos\vartheta \quad (-\pi\leqq\vartheta\leqq\pi)\,, \\ y_p&=g(\vartheta)=g_1(\vartheta)+g_2(\vartheta) \\ &\qquad +g_3(\vartheta)+O(t^4)\,, \end{aligned}\right\} \tag{3.1}$$

where

$$\left.\begin{aligned} g_1(\vartheta)&=\pm\frac{t}{2}(1-\cos 2\vartheta)\,, \\ g_2(\vartheta)&=0\,, \\ g_3(\vartheta)&=\pm\frac{t^3}{8}(1-\cos 4\vartheta)\,. \end{aligned}\right\} \tag{3.2}$$

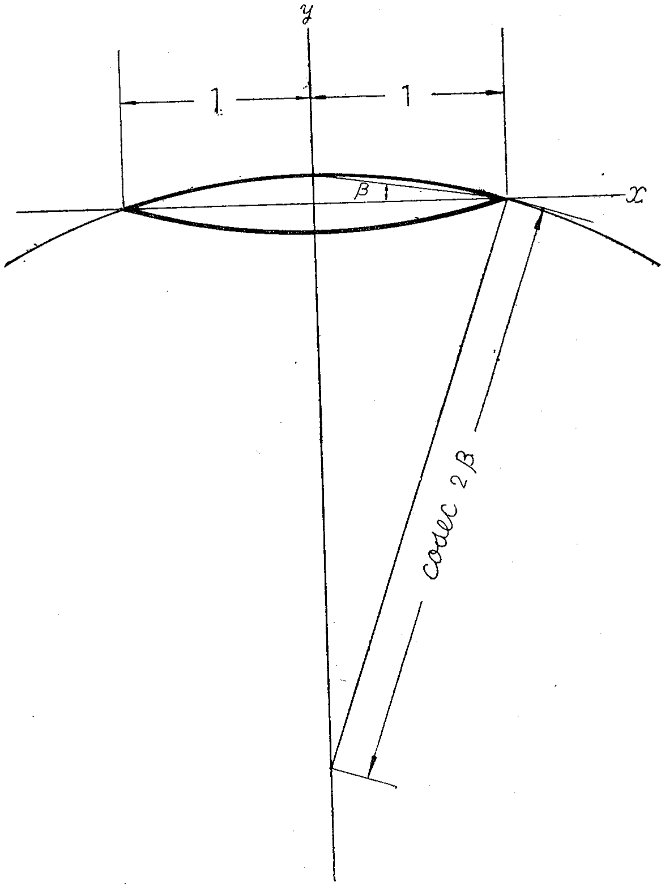

Fig. 1.

In these expressions, we shall take the upper sign (+) for the upper surface ($0\leqq\vartheta\leqq\pi$), and the lower sign (−) for the lower surface ($0\geqq\vartheta\geqq-\pi$). Thanks to this notation, manipulation of infinite series in ϑ may be avoided even in the case of profiles with finite edge angles.

We must first obtain the conjugate Fourier series for $g(\theta)$. The formula I–(3.17) is favourable for this purpose. For example,

$$\begin{aligned} g_1^*(\theta)&=-\frac{1}{2\pi}\left\{\int_0^\pi \frac{t}{2}(1-\cos 2\varphi)\cot\frac{\varphi-\theta}{2}\,d\varphi\right. \\ &\qquad\qquad \left.-\int_{-\pi}^0 \frac{t}{2}(1-\cos 2\varphi)\cot\frac{\varphi-\theta}{2}\,d\varphi\right\} \\ &=-\frac{t}{\pi}\left\{2\cos\theta-(1-\cos 2\theta)\log\left|\tan\frac{\theta}{2}\right|\right\}\,. \end{aligned}$$

The factor $\log|\tan(\theta/2)|$ will appear so frequently throughout this analysis, that it is convenient to adopt the simple notations

$$l(\theta)\equiv\log\left|\tan\frac{\theta}{2}\right|, \quad l^2(\theta)\equiv\left(\log\left|\tan\frac{\theta}{2}\right|\right)^2, \quad l^3(\theta)\equiv\left(\log\left|\tan\frac{\theta}{2}\right|\right)^3. \tag{3.3}$$

Then

$$\left.\begin{aligned}
&g_1^*(\theta)=-\frac{t}{\pi}\{2\cos\theta-(1-\cos 2\theta)l(\theta)\}\ ,\\
&\text{and similarly}\\
&g_3^*(\theta)=-\frac{t^3}{\pi}\left\{\frac{2}{3}\cos\theta+2\cos 3\theta-(1-\cos 4\theta)l(\theta)\right\}\ .
\end{aligned}\right\} \tag{3.4}$$

Substituting from (3.2) and (3.4) into the formulae I-(4.13), the mapping function correct to the order of t^3 is obtained as follows:

$$\left.\begin{aligned}
\eta_1(\theta)&=\pm\, t\mu\frac{1}{2}(1-\cos 2\theta)\ ,\\
\xi_1(\theta)&=\quad t\mu\frac{1}{\pi}(1-\cos 2\theta)l(\theta)\ ,\\
\eta_2(\theta)&=\mp\, t^2\mu^2\frac{1}{\pi}(\cos\theta-\cos 3\theta)l(\theta)\ ,\\
\xi_2(\theta)&=-\,t^2\mu^2\frac{1}{\pi^2}(\cos\theta-\cos 3\theta)\left(l^2(\theta)-\frac{\pi^2}{4}\right),\\
\eta_3(\theta)&=\mp\, t^3\mu^3\frac{1}{2\pi^2}\left\{(1-\cos 4\theta)\frac{\pi^2}{4}l(\theta)+(1-4\cos 2\theta+3\cos 4\theta)l^2(\theta)\right\}\\
&\quad\pm t^3\mu M^2\frac{1}{8}(1-\cos 4\,\theta)\ ,\\
\xi_3(\theta)&=-\,t^3\mu^3\frac{1}{3\pi^3}\left\{(1+8\cos 2\theta-9\cos 4\theta)\frac{\pi^2}{4}l(\theta)\right.\\
&\quad\left.+(1-4\cos 2\theta+3\cos 4\theta)l^3(\theta)\right\}\\
&\quad+t^3\mu M^2\frac{1}{4\pi}\{2(\cos\theta-\cos 3\theta)+(1-\cos 4\theta)l(\theta)\}\ .
\end{aligned}\right\} \tag{3.5}$$

§ 4. Velocity Potential

The first approximation. The equation I-(3.3) is rewritten in the form:

$$G_1=f(\theta)=-\frac{1}{\mu^2}(\eta_1^*(\theta)+i\eta_1(\theta))\ .$$

Then we get for the profile considered,

$$f(\theta)=\frac{t}{\mu}\frac{1}{\pi}\left[\{2\cos\theta-(1-\cos 2\theta)l(\theta)\}\mp i\frac{\pi}{2}(1-\cos 2\theta)\right]. \tag{4.1}$$

Evidently $f(\theta)$ satisfies the conditions (ii) and (iii) assigned for G_1. But

$$\frac{df}{d\theta}=-\frac{t}{\mu}\frac{4}{\pi}\sin\theta\left\{(1+\cos\theta\, l(\theta))\pm i\frac{\pi}{2}\cos\theta\right\}\ ,$$

and $\dfrac{d\zeta}{d\theta}=O((\sin\theta)^{1-\varepsilon})$ as θ tends to 0 or π, since the profile in the ζ-

plane has the finite edge angle $4\mu\beta$ ($\varepsilon=4\mu\beta/\pi$). Therefore $\frac{df}{d\zeta}=\frac{df(\theta)}{d\theta}\Big/\frac{d\zeta}{d\theta}$ vanishes at $\theta=0$ or π; that is, $f(\theta)$ satisfies also the condition (i). Taking this fact into account, we shall put in later calculations

$$\frac{df}{d\zeta}=\frac{t}{\mu}\frac{4}{\pi}\left\{(1+\cos\theta\, l(\theta))\pm i\frac{\pi}{2}\cos\theta\right\} \tag{4.2}$$

as the first approximation.

Hence $f(\theta)$ is certainly the required first approximation for G, and its real part gives $\phi_1(\theta)$.

The second approximation. f_2^0 is determined in a similar way:

$$f_2^0=t^2\frac{2}{\pi^2}\left[\left\{2\cos\theta+\frac{1}{2}(\cos\theta-\cos 3\theta)\left(l^2(\theta)-\frac{\pi^2}{4}\right)\right\}\right.$$
$$\left.\pm i\frac{\pi}{2}(\cos\theta-\cos 3\theta)l(\theta)\right]. \tag{4.3}$$

The pair of g_2^1 and f_2^1 does not contribute to the value of G_2 on the surface, so that we can save its calculation.

$$\left.\begin{aligned}
g_2^2=\frac{df}{d\zeta}\bar{f}=\frac{t^2}{\mu^2}\frac{8}{\pi^2}\Bigg[&\Bigg\{\cos\theta+\cos 2\theta\, l(\theta)\\
&-\frac{1}{4}(\cos\theta-\cos 3\theta)\left(l^2(\theta)+\frac{\pi^2}{4}\right)\Bigg\}\pm i\frac{\pi}{2}\Bigg],\\
\text{and}\qquad & \\
f_2^2=-\frac{t^2}{\mu^2}\frac{8}{\pi^2}&\left\{l(\theta)\pm i\frac{\pi}{2}\right\},
\end{aligned}\right\} \tag{4.4}$$

since the conjugate Fourier series for $\pm\pi/2$ is just equal to $l(\theta)$.

Further,

$$\left.\begin{aligned}
g_2^3&=\overline{f_2^3},\\
f_2^3&=\int\left(\frac{df}{d\zeta}\right)^2 d\zeta=\int\left(\frac{df}{d\zeta}\right)^2(-\sin\theta)d\theta\\
&=\frac{t^2}{\mu^2}\frac{4}{3\pi^2}\Bigg[\Bigg\{4\cos\theta-\frac{\pi^2}{4}(3\cos\theta+\cos 3\theta)-4(1-\cos 2\theta)l(\theta)\\
&\quad-(\cos\theta-\cos 3\theta)l^2(\theta)-4s_2(\theta)\Bigg\}\pm i\pi\{2\cos 2\theta\\
&\quad-(\cos\theta-\cos 3\theta)l(\theta)-4s_1(\theta)\}\Bigg].
\end{aligned}\right\} \tag{4.5}$$

In this expression, we have put

$$\left.\begin{aligned} s_1(\theta) &= \int_0^\theta \sin\theta\, l(\theta) d\theta\ , \\ s_2(\theta) &= \int_0^\theta \sin\theta\, l^2(\theta) d\theta\ , \\ s_3(\theta) &= \int_0^\theta \sin\theta\, l^3(\theta) d\theta\ . \end{aligned}\right\} \qquad (4.6)^{3)}$$

$s_3(\theta)$ will appear later in the expression for G_3.

The G_2 is the linear combination of (4.3), (4.4) and (4.5) as expressed in I–(3.4) and I–(3.5), that is

$$G_2 = f_2^0 + \frac{M^2}{4}(1+\nu)\{2(g_2^2+f_2^2)+(g_2^3+f_2^3)\}\ . \qquad (4.7)$$

The second approximation of the velocity potential, $\phi_2(\theta)$, is the real part of G_2.

The third approximation. g_3^j and f_3^j can be obtained quite similarly to g_2^j and f_2^j. The calculations for G_3 are so lengthy that their final expressions have been summarized in Appendix B.

§ 5. Velocity Distribution

So far we have determined the mapping function and the potential function for a symmetrical circular arc aerofoil correct to the order of t^3. Now we are ready to compute the velocity distribution over the surface of the aerofoil correct to the same order. We may use any one of the formulae described in § 5 of Part I. Among those formulae, I–(5.8) expressed in terms of ϑ is very convenient for practical computations. It is because that the value of ϑ corresponding to a definite point on the surface of an aerofoil is fixed, while that of θ corresponding to the same point varies as the thickness and the Mach number of the undisturbed flow increase. By making use of the formulae I–(5.8), we have obtained the following expressions for the velocity distribution:

$$q(\vartheta) = 1 + q_{\mathrm{I}}(\vartheta) + q_{\mathrm{II}}(\vartheta) + q_{\mathrm{III}}(\vartheta) + O(t^4)\ , \qquad (5.1)$$

where

$$q_{\mathrm{I}}(\vartheta) = t\,\frac{1}{\mu}(1+\cos\vartheta\, l(\vartheta))\,, \qquad (5.2)$$

$$\begin{aligned} q_{\mathrm{II}}(\vartheta) = {} & t^2\Big[-\frac{1}{2}(1-\cos 2\vartheta) + \frac{2}{\pi^2}\{6(1+2\cos\vartheta\, l(\vartheta)) + (1+3\cos 2\vartheta) l^2(\vartheta)\}\Big] \\ & + t^2\frac{M^2}{\mu^2}(1+\nu)\Big[-\frac{1}{2}(1-\cos 2\vartheta) + \frac{2}{\pi^2}\{10(1+2\cos\vartheta\, l(\vartheta)) \\ & + (3+5\cos 2\vartheta) l^2(\vartheta)\}\Big]\,, \end{aligned} \qquad (5.3)$$

---

3) $s_1(\theta)$ can be expressed in terms of the known functions:

$$s_1(\theta) = \log|\sin\theta| - \cos\theta\, l(\theta) - \log 2\,,$$

while $s_2(\theta)$ and $s_3(\theta)$ are newly defined functions.

$$
\begin{aligned}
q_{\mathrm{III}}(\vartheta)= t^3\frac{1}{\mu}\Big[&-\frac{2}{3\pi}\{2(1-3\cos 2\vartheta)+(5\cos\vartheta-3\cos 3\vartheta)\,l(\vartheta)\}\\
&+\frac{8}{3\pi^3}\{12(1+3\cos\vartheta\, l(\vartheta))+6(1+3\cos 2\vartheta)l^2(\vartheta)\\
&+(\cos\vartheta+\cos 3\vartheta)l^3(\vartheta)\}\Big]\\
+t^3\frac{M^2}{\mu}\Big[&\frac{2}{3\pi}\Big\{\Big(\frac{2}{3}-2\cos 2\vartheta\Big)+(\cos\vartheta-\cos 3\vartheta)l(\vartheta)\Big\}\\
&-\frac{8}{3\pi^3}\{4(1+3\cos\vartheta\, l(\vartheta))+6\cos 2\vartheta\, l^2(\vartheta)-(\cos\vartheta-\cos 3\vartheta)l^3(\vartheta)\}\Big]\\
+t^3\frac{M^2}{\mu}(1+\nu)\Big[&\frac{1}{3\pi}\Big\{10\Big(\frac{5}{3}+\cos 2\vartheta\Big)-(21\cos\vartheta-5\cos 3\vartheta)l(\vartheta)\Big\}\\
&+\frac{4}{3\pi^3}\{68(1+3\cos\vartheta\, l(\vartheta))+2(27+51\cos 2\vartheta)l^2(\vartheta)\\
&+(15\cos\vartheta+17\cos 3\vartheta)l^3(\vartheta)\}\Big]\\
+t^3\frac{M^4}{\mu^3}\{(3\gamma+5)&+2(2\gamma+7)\nu+12\nu^2\}\Big[\frac{1}{3\pi}\Big\{\Big(\frac{1}{3}+2\cos 2\vartheta\Big)\\
&+(\cos\vartheta+\cos 3\vartheta)l(\vartheta)\Big\}+\frac{4}{3\pi^3}\{4(1+3\cos\vartheta\, l(\vartheta))\\
&+3(1+2\cos 2\vartheta)l^2(\vartheta)+(\cos\vartheta+\cos 3\vartheta)l^3(\vartheta)\}\Big]\\
+t^3\frac{M^2}{\mu^3}\Big[&1+\frac{M^2}{2}\{2(\gamma+1)+(2\gamma+9)\nu+7\nu^2\}\Big]\\
&\times\Big[\frac{8}{9\pi}\Big\{\Big(\frac{1}{1+\cos\vartheta}+\frac{2}{3}+4\cos 2\vartheta\Big)\\
&+\Big(\frac{1}{2}+3\cos\vartheta+2\cos 3\vartheta\Big)l(\vartheta)-3s_1(\vartheta)\Big\}\\
&+\frac{32}{9\pi^3}\Big\{8(1+3\cos\vartheta\, l(\vartheta))+3(3+4\cos 2\vartheta)l^2(\vartheta)\\
&+2(2\cos\vartheta+\cos 3\vartheta)l^3(\vartheta)+6\frac{\cos\vartheta}{1-\cos 2\vartheta}s_2(\vartheta)-3l(\vartheta)s_2(\vartheta)\\
&+(s_3(\vartheta)+\sigma_3)\Big\}\Big]\\
+t^3\frac{M^4}{\mu^3}\{3(\gamma+3)&+2(2\gamma+11)\nu+16\nu^2\}\Big[-\frac{1}{\pi}\{2(1+\cos 2\vartheta)\\
&+(3\cos\vartheta+\cos 3\vartheta)l(\vartheta)\}+\frac{4}{3\pi^3}\{4(1+3\cos\vartheta\, l(\vartheta))
\end{aligned}
$$

$$+6(1+\cos 2\vartheta)l^2(\vartheta)+(3\cos\vartheta+\cos 3\vartheta)l^3(\vartheta)\}\Big]$$

$$+t^3\frac{M^4}{\mu^3}(1+\nu)^2\Big[\frac{2}{3\pi}\Big\{\Big(\frac{25}{6}+\frac{29}{2}\cos 2\vartheta\Big)+(3\cos\vartheta+5\cos 3\vartheta)l(\vartheta)\Big\}$$

$$+\frac{8}{3\pi^3}\{20(1+3\cos\vartheta\, l(\vartheta))+15(1+2\cos 2\vartheta)l^2(\vartheta)$$

$$+(3\cos\vartheta+5\cos 3\vartheta)l^3(\vartheta)\}\Big]. \tag{5.4}$$

The meanings of the notations used here are as follows:

M: Mach number of the undisturbed flow,

γ: ratio of the specific heats (for standard air $\gamma=1.40$),

$\mu=\sqrt{1-M^2}$, $\nu=\frac{\gamma+1}{4}\frac{M^2}{\mu^2}$, $\sigma_3=-1.8030\ 8535$ (cf. Appendix A).

These formulae cannot be applied for regions near the leading and the trailing edge, where the expressions for q diverge. For these regions q must be calculated by the formula I-(5.2) or I-(5.8).

The velocity distribution for our profile obtained by the thin-wing-expansion method is always symmetrical fore and aft. The maximum velocity seems to occur at the mid-chord point unless a shock wave appears. This maximum velocity is evaluated by putting $\vartheta=\pi/2$ in (5.1)$\sim$(5.4) as follows:

$$q_{\max}=1+t\frac{1}{\mu}\frac{4}{\pi}+t^2\Big\{\Big(-1+\frac{12}{\pi^2}\Big)+\frac{M^2}{\mu^2}(1+\nu)\Big(-1+\frac{20}{\pi^2}\Big)\Big\}$$

$$+t^3\Big\{\frac{1}{\mu}\Big(-\frac{16}{3\pi}+\frac{32}{\pi^3}\Big)+\frac{M^2}{\mu}\Big(\frac{16}{9\pi}-\frac{32}{3\pi^3}\Big)+\frac{M^2}{\mu}(1+\nu)\Big(\frac{20}{9\pi}+\frac{272}{3\pi^3}\Big)$$

$$+\frac{M^4}{\mu^3}\{(3\gamma+5)+2(2\gamma+7)\nu+12\nu^2\}\Big(-\frac{5}{9\pi}+\frac{16}{3\pi^3}\Big)$$

$$+\frac{M^2}{\mu^3}\Big[1+\frac{M^2}{2}\{2(\gamma+1)+(2\gamma+9)\nu+7\nu^2\}\Big]$$

$$\times\Big(-\frac{56}{27\pi}+\frac{8}{3\pi}\log 2+\frac{256}{9\pi^3}+\frac{56}{9\pi^3}\sigma_3\Big)$$

$$+\frac{M^4}{\mu^3}\{3(\gamma+3)+2(2\gamma+11)\nu+16\nu^2\}\frac{16}{3\pi^3}+\frac{M^4}{\mu^3}(1+\nu)^2\Big(-\frac{62}{9\pi}+\frac{160}{3\pi^3}\Big)\Big\}$$

$$+O(t^4). \tag{5.5}$$

§ 6. Numerical Results and Discussions

The velocity distributions over the surface of the symmetrical circular arc aerofoil of the thickness ratio $t=0.1$, have been computed for various Mach numbers.

For the flow of an incompressible fluid, the velocity distribution for this aerofoil can be determined by means of the well known formula of the von Kármán-Trefftz transformation. In Appendix C, the results by the thin-wing-expansion method are compared with this exact solution, and the accuracy of these approximations has been found satisfactory. It seems to be generally accepted that the thin-wing-expansion method would be applied successfully for the problems, which necessitate the conformal transformation of the region of slender shape into a circle.

Table I. Velocity Distributions over the Surface of a Symmetrical Circular Arc Aerofoil $t=0.1$.

		$M=0.6$			$M=0.7$			$M=0.8$		
ϑ (deg.)	x	q^{I}	q^{II}	q^{III}	q^{I}	q^{II}	q^{III}	q^{I}	q^{II}	q^{III}
9	0.988	0.760	0.776	0.770	0.731	0.762	0.725	0.679	0.753	0.530
18	0.951	0.880	0.870	0.870	0.866	0.853	0.840	0.840	0.822	0.724
27	0.891	0.957	0.941	0.941	0.952	0.929	0.919	0.942	0.901	0.828
36	0.809	1.014	1.000	0.999	1.016	0.995	0.987	1.019	0.980	0.921
45	0.707	1.060	1.050	1.049	1.067	1.053	1.047	1.080	1.054	1.011
54	0.588	1.096	1.091	1.092	1.108	1.102	1.100	1.128	1.120	1.098
63	0.454	1.124	1.125	1.126	1.139	1.142	1.144	1.165	1.176	1.175
72	0.309	1.143	1.149	1.151	1.161	1.172	1.178	1.191	1.217	1.237
81	0.156	1.156	1.165	1.168	1.174	1.190	1.196	1.207	1.243	1.275
90	0	1.159	1.169	1.172	1.178	1.196	1.205	1.212	1.252	1.288

q^{I}.....1st approx. q^{II}.....2nd approx. q^{III}.....3rd approx.

The numerical values of the magnitude of the velocity at the surface of the profile are listed in Table I and their distribution curves are shown in Figs. 2, 3 and 4.

It may be noted, that the velocity distribution curves do not present any peculiarity, such as seen in the case of an elliptic cylinder,[2] even at the point $\vartheta=9°$ and up to the value of $M=0.8$.

Comparing these curves, it seems probable that the process of iteration would converge at and below the Mach number $M=0.7$, but diverge at $M=0.8$. On the other hand, there is no supersonic region on the surface when $M\leqq 0.7$, while the fluid velocities in some region near the mid-chord point exceed the local speed of sound at $M=0.8$. In order to make the situation more obvious, the maximum velocities

q_{max} calculated by making use of (5.5) are plotted against Mach numbers for each step of approximation in Fig. 5. In this figure the curve of the critical speed q_{cr}, which coincides with the local speed of sound, is also included.

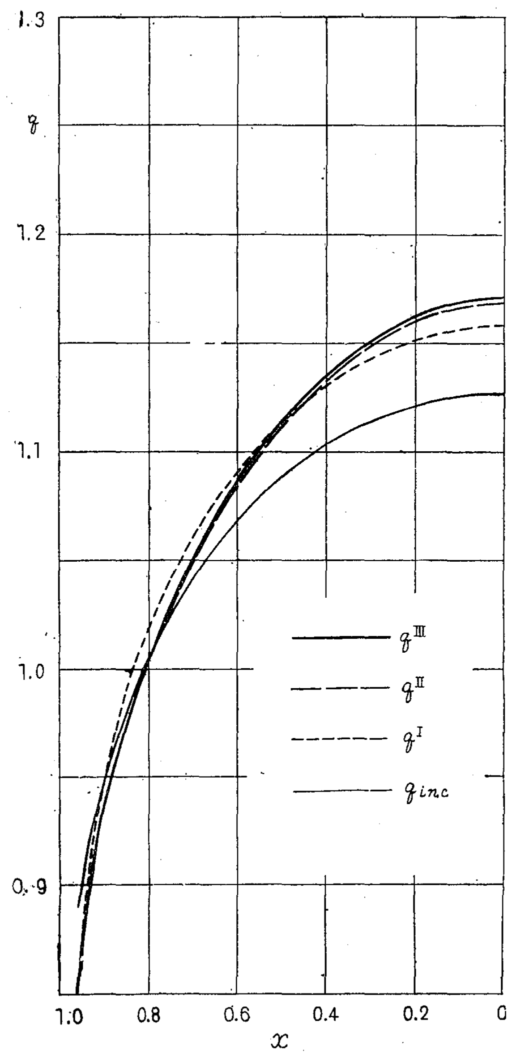

Fig. 2. Velocity distribution over the surface of a symmetrical circular arc aerofoil, $t=0.1$, $M=0.6$.

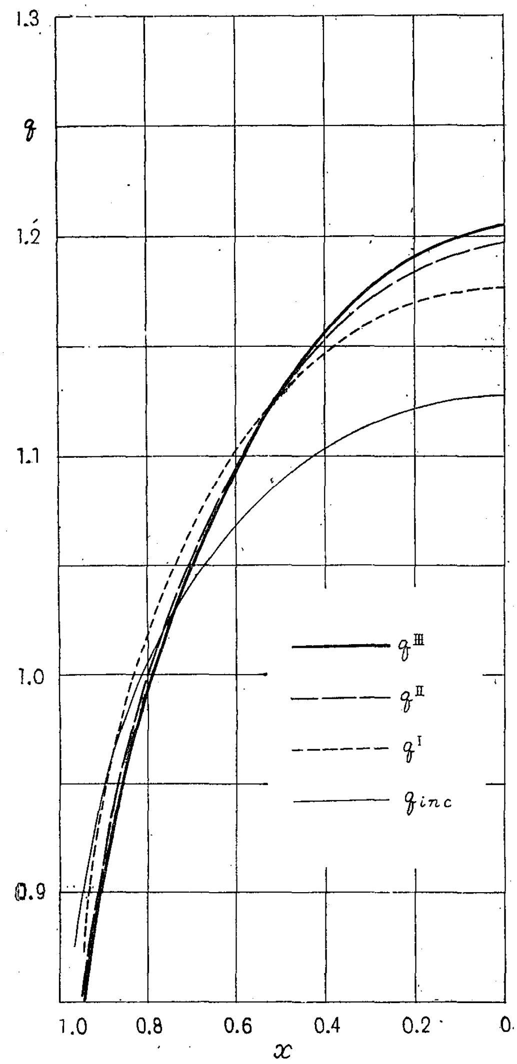

Fig. 3. Velocity distribution over the surface of a symmetrical circular arc aerofoil, $t=0.1$, $M=0.7$.

Here we may consider two kinds of critical Mach numbers. The critical Mach number of the first kind is defined as that of the undisturbed flow at which the continuous potential flow past an aerofoil first breaks down. The critical Mach number of the second kind is defined as that of the undisturbed flow at which the local fluid velocity first attains the local speed of sound somewhere in the flow. Comparing the curves in Fig. 5, the following conjecture would seem plausible: The critical Mach number of the first kind and that of the second kind would coincide with each other. In this regard, however, our present informations are far from complete and further investigations are necessary.

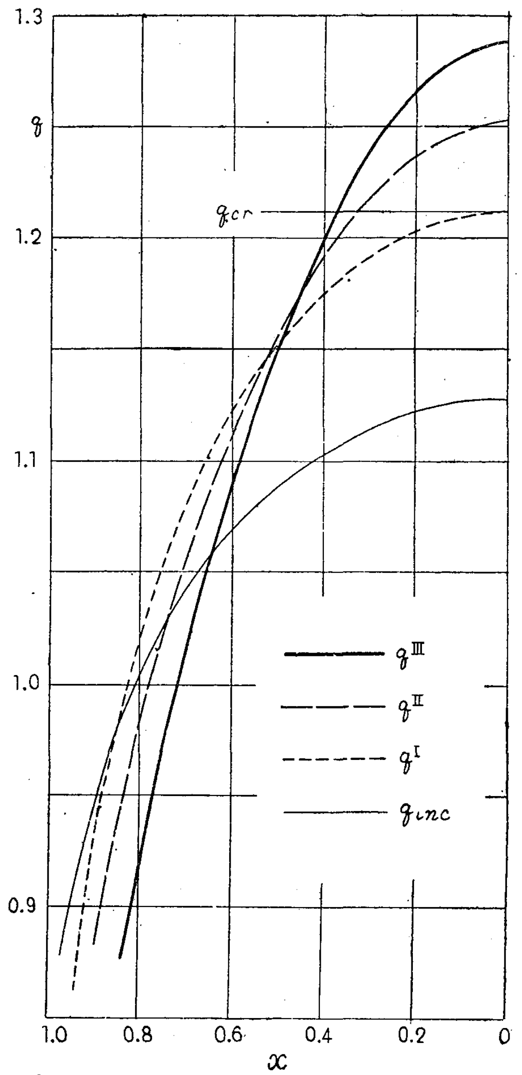

Fig. 4. Velocity distribution over the surface of a symmetrical circular arc aerofoil, $t=0.1$, $M=0.8$.

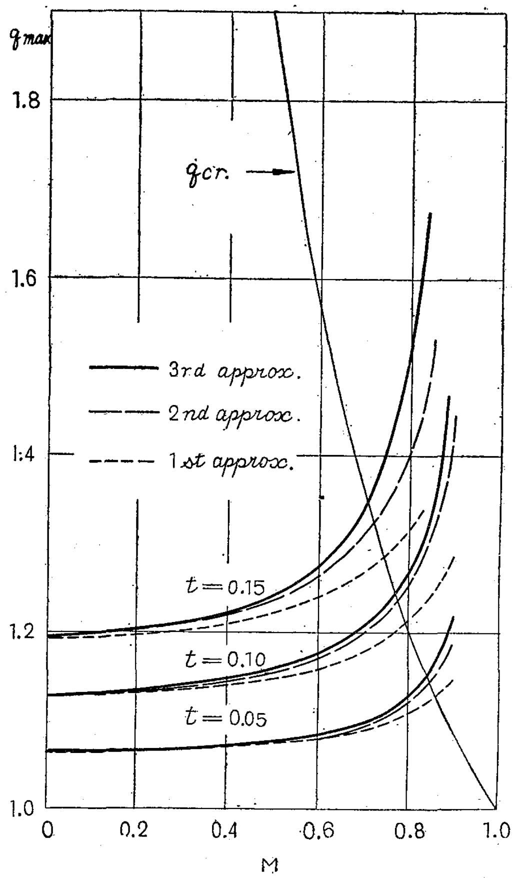

Fig. 5. Maximum velocity at the surface of a symmetrical circular arc aerofoils.

It is very interesting to discuss about the results stated above, comparing them with those of the observations in the actual flow, or with the results of resembling aerofoils, e.g. an elliptic cylinder, a circular arc aerofoil with infinitesimal thickness, etc. We will report on these subjects in a separate paper.

Here the author wishes to express his hearty thanks to Prof. I. Imai for his suggestions and advices throughout this work. He is also indebted to Mr. W. Motizuki for the help in preparation of the manuscript of this paper.

Appendices

A. The Conjugate Fourier Series

In this analysis, it is necessary to determine the conjugate Fourier series for the functions such as $\cos n\theta\, F(\theta)$. The $F(\theta)$'s are ± 1 (that is 1 for $0<\theta<\pi$ and -1 for $0>\theta>-\pi$), $\pm l(\theta)$, $\pm l^2(\theta)$ and others.

Here the integral formula I-(3.17)

$$R^*(\theta)=-\frac{1}{2\pi}\int_{-\pi}^{\pi} R(\varphi)\cot\frac{\varphi-\theta}{2}d\varphi\ ,$$

is favourable. By making use of recurrence formulae, we can reduce $\int \cos n\varphi\, F(\varphi)\cot\frac{\varphi-\theta}{2}d\varphi$ into $\int F(\varphi)\cot\frac{\varphi-\theta}{2}d\varphi$, $\int F(\varphi)d\varphi$ and $\int \sin n\varphi\, F(\varphi)d\varphi$; that is

$$\begin{aligned}&\int \cos n\varphi\, F(\varphi)\cot\frac{\varphi-\theta}{2}d\varphi\\ &=\cos n\theta\int F(\varphi)\cot\frac{\varphi-\theta}{2}d\varphi-\sin n\theta\int F(\varphi)d\varphi\\ &\quad-2\sum_{p=1}^{n-1}\int\sin\{(n-p)\theta+p\varphi\}F(\varphi)d\varphi-\int\sin n\varphi F(\varphi)d\varphi\ . \qquad \text{(A.1)}\end{aligned}$$

Then it is concluded that $[\cos n\theta\, F(\theta)]^*$ exists if $F(\theta)$ is integrable in the range $-\pi\leqq\theta\leqq\pi$ though $F(\theta)$ has some singularities.

We put $F(\theta)=\pm 1$, then

$$\begin{aligned}[\pm 1]^*&=-\frac{1}{2\pi}\left\{\int_0^{\pi}\cot\frac{\varphi-\theta}{2}d\varphi-\int_{-\pi}^{0}\cot\frac{\varphi-\theta}{2}d\varphi\right\}\\ &=\frac{2}{\pi}\log\left|\tan\frac{\theta}{2}\right|\equiv\frac{2}{\pi}l(\theta)\ . \qquad \text{(A.2)}\end{aligned}$$

By virtue of (A.1),

$$\left.\begin{aligned}[\pm\cos\theta]^*&=\frac{2}{\pi}\{1+\cos\theta\, l(\theta)\}\ ,\\ [\pm\cos 2\theta]^*&=\frac{2}{\pi}\{2\cos\theta+\cos 2\theta\, l(\theta)\}\ ,\\ [\pm\cos 3\theta]^*&=\frac{2}{\pi}\left\{\frac{1}{3}+2\cos 2\theta+\cos 3\theta\, l(\theta)\right\}\ ,\\ [\pm\cos 4\theta]^*&=\frac{2}{\pi}\left\{\frac{2}{3}\cos\theta+2\cos 3\theta+\cos 4\theta\, l(\theta)\right\}\ .\end{aligned}\right\} \qquad \text{(A.3)}$$

In the case when $F(\theta)=\pm l(\theta)$,

$$
\begin{aligned}
[\pm l(\theta)]^* &= -\frac{1}{2\pi}\left\{\int_0^{\pi} l(\theta)\cot\frac{\varphi-\theta}{2}\,d\varphi - \int_{-\pi}^{0} l(\theta)\cot\frac{\varphi-\theta}{2}\,d\varphi\right\} \\
&= -\frac{1}{2\pi}\int_0^{\pi/2}\log\left|\tan\frac{\theta}{2}\right|\frac{4\sin 2\varphi}{\cos 2\theta-\cos 2\varphi}\,d\varphi \\
&= \frac{1}{\pi}\left(l^2(\theta)-\frac{\pi^2}{4}\right).
\end{aligned}
\tag{A.4}
$$

By making use of (A.1) again, we can get

$$
\left.
\begin{aligned}
[\pm\cos\theta\, l(\theta)]^* &= \frac{1}{\pi}\cos\theta\left(l^2(\theta)-\frac{\pi^2}{4}\right), \\
[\pm\cos 2\theta\, l(\theta)]^* &= \frac{1}{\pi}\left\{-2+\cos 2\theta\left(l^2(\theta)-\frac{\pi^2}{4}\right)\right\}, \\
[\pm\cos 3\theta\, l(\theta)]^* &= \frac{1}{\pi}\left\{-4\cos\theta+\cos 3\theta\left(l^2(\theta)-\frac{\pi^2}{4}\right)\right\}.
\end{aligned}
\right\}
\tag{A.5}
$$

Other conjugate Fourier series necessary for the calculations of G_2 and G_3 are obtained by the similar treatments as follows:

$$
\left.
\begin{aligned}
[\pm l^2(\theta)]^* &= \frac{2}{3\pi}\left(l^3(\theta)-\frac{\pi^2}{2}l(\theta)\right), \\
[\pm\cos\theta\, l^2(\theta)]^* &= \frac{2}{3\pi}\left\{\frac{\pi^2}{4}+\cos\theta\left(l^3(\theta)-\frac{\pi^2}{2}l(\theta)\right)\right\}, \\
[\pm\cos 2\theta\, l^2(\theta)]^* &= \frac{2}{3\pi}\left\{\frac{\pi^2}{2}\cos\theta+\cos 2\theta\left(l^3(\theta)-\frac{\pi^2}{2}l(\theta)\right)\right\}, \\
[\pm\cos 3\theta\, l^2(\theta)]^* &= \frac{2}{3\pi}\left\{\left(4+\frac{\pi^2}{12}\right)+\frac{\pi^2}{2}\cos 2\theta\right. \\
&\qquad\left.+\cos 3\theta\left(l^3(\theta)-\frac{\pi^2}{2}l(\theta)\right)\right\}, \\
[\pm\cos 4\theta\, l^2(\theta)]^* &= \frac{2}{3\pi}\left\{\left(8+\frac{\pi^2}{6}\right)\cos\theta+\frac{\pi^2}{2}\cos 3\theta\right. \\
&\qquad\left.+\cos 4\theta\left(l^3(\theta)-\frac{\pi^2}{2}l(\theta)\right)\right\};
\end{aligned}
\right\}
\tag{A.6}
$$

$$
\left.
\begin{aligned}
[\pm s_1(\theta)]^* &= \frac{1}{\pi}\left\{-\frac{\pi^2}{4}(1-\cos\theta)+(s_2(\theta)+\sigma_2)\right\}, \\
[\pm s_2(\theta)]^* &= \frac{2}{3\pi}\left\{-\frac{\pi^2}{4}+\frac{\pi^2}{4}(1-\cos\theta)\,l(\theta)\right. \\
&\qquad\left.-\frac{3\pi^2}{4}s_1(\theta)+(s_3(\theta)+\sigma_3)\right\}, \\
[\pm\cos\theta\, s_2(\theta)]^* &= \frac{2}{3\pi}\left\{\frac{\pi^2}{4}(1-\cos\theta)+\frac{\pi^2}{4}(1-\cos\theta)\cos\theta\, l(\theta)\right. \\
&\qquad\left.-\frac{3\pi^2}{4}\cos\theta\, s_1(\theta)+\cos\theta(s_3(\theta)+\sigma_3)\right\},
\end{aligned}
\right.
\tag{A.7}
$$

$$[\pm\cos\theta\, l(\theta)s_1(\theta)]^* = \frac{1}{\pi}\left\{-\frac{\pi^2}{6}\cos\theta - \frac{\pi^2}{12}(1-\cos\theta)\cos\theta\, l(\theta)\right.$$
$$-\frac{\pi^2}{4}\cos\theta\, s_1(\theta) + \cos\theta\, l(\theta)s_2(\theta)$$
$$\left.-\frac{1}{3}\cos\theta\,(s_3(\theta)+\sigma_3)\right\}.$$

Here σ_2 and σ_3 are the constants defined as

$$\sigma_2 = -\int_0^1 \frac{\log x}{1-x}\,dx = \frac{\pi^2}{6} = 1.6449\ 3407\ ,$$
$$\sigma_3 = -\frac{3}{4}\int_0^1 \frac{(\log x)^2}{1-x}\,dx = -\frac{3}{2}\zeta(3) = -1.8030\ 8535\ ,$$

where $\zeta(z)$ is Riemann's ζ-function.

The above formulae for the conjugate Fourier series can be obtained more directly on the basis of the theory of functions. But the calculations in this section may be useful as an example for analysis of commonly used aerofoils.

B. Expressions for G_3

g_3^j and f_3^j are as follows:

$$f_3^0 = t^3\mu\frac{1}{3\pi^3}\left[\left\{(24-2\pi^2)\cos\theta + (1-\cos 2\theta)\pi^2 l(\theta)\right.\right.$$
$$\left. + (1-4\cos 2\theta + 3\cos 4\theta)\left(l^3(\theta) - \frac{3\pi^2}{4}l(\theta)\right)\right\}$$
$$\left.\pm i\frac{\pi}{2}\left\{\pi^2(1-\cos 2\theta) + (1-4\cos 2\theta + 3\cos 4\theta)\left(3l^2(\theta) - \frac{\pi^2}{4}\right)\right\}\right]$$
$$+ t^3\frac{M^2}{\mu}\frac{1}{4\pi}\left[\left\{\frac{2}{3}\cos\theta + 2\cos 3\theta - (1-\cos 4\theta)l(\theta)\right\} \mp i\frac{\pi}{2}(1-\cos 4\theta)\right],$$

$$g_3^1 = \frac{t^3}{\mu}\frac{4}{\pi^3}\left[\left\{4(1-\cos 2\theta)l(\theta) + 4(\cos\theta - \cos 3\theta)\left(l^2(\theta) + \frac{\pi^2}{4}\right)\right.\right.$$
$$\left. + (1-\cos 4\theta)\left(l^3(\theta) + \frac{\pi^2}{4}l(\theta)\right)\right\}$$
$$\left.\mp i\frac{\pi}{2}\left\{4(1-\cos 2\theta) - (1-\cos 4\theta)\left(l^2(\theta) + \frac{\pi^2}{4}\right)\right\}\right],$$

$$f_3^1 = \frac{t^3}{\mu}\frac{4}{\pi^3}\left\{\left(-\frac{16}{3} + \frac{2\pi^2}{9}\right)\cos\theta + \frac{2\pi^2}{3}\cos 3\theta + 4(1-\cos 2\theta)l(\theta)\right.$$
$$\left. -\frac{1}{3}(1-\cos 4\theta)\left(l^3(\theta) + \frac{\pi^2}{4}l(\theta)\right)\right\} - i\Im(g_3^1)\ ,$$

$$g_3^3 = -\frac{t^3}{\mu}\frac{4}{\pi^3}\left[\left\{\left(4 + \frac{15\pi^2}{4}\right)\cos\theta + \frac{\pi^2}{4}\cos 3\theta + 4(1+2\cos 2\theta)l(\theta)\right.\right.$$

$$+(3\cos\theta+5\cos 3\theta)l^2(\theta)-(1-\cos 4\theta)\left(l^3(\theta)+\frac{\pi^2}{4}l(\theta)\right)\Big\}$$

$$\pm i\frac{\pi}{2}\Big\{4(2+\cos 2\theta)+4(3\cos\theta+\cos 3\theta)l(\theta)-(1-\cos 4\theta)\left(l^2(\theta)+\frac{\pi^2}{4}\right)\Big\}\Big],$$

$$f_3^3=\frac{t^3}{\mu}\frac{4}{\pi^3}\Big\{\left(\frac{8}{3}+\frac{2\pi^2}{9}\right)\cos\theta+\frac{2\pi^2}{3}\cos 3\theta+4(2+\cos 2\theta)l(\theta)$$

$$+2(3\cos\theta+\cos 3\theta)\left(l^2(\theta)-\frac{\pi^2}{4}\right)$$

$$-\frac{1}{3}(1-\cos 4\theta)\left(l^3(\theta)+\frac{\pi^2}{4}l(\theta)\right)\Big\}-i\Im(g_3^3)\ ,$$

$$g_3^4=\overline{f_3^4},$$

$$f_3^4=-\frac{t^3}{\mu}\frac{2}{3\pi^3}\Big[\Big\{8\cos\theta-4\pi^2(1-\cos\theta)-20(1-\cos 2\theta)l(\theta)$$

$$-14(\cos\theta-\cos 3\theta)\left(l^2(\theta)-\frac{\pi^2}{4}\right)+16(s_2(\theta)+\sigma_2)$$

$$-3(5-4\cos 2\theta-\cos 4\theta)\left(l^3(\theta)-\frac{3\pi^2}{4}l(\theta)\right)\Big\}$$

$$\pm i\frac{\pi}{2}\Big\{-20(1-\cos 2\theta)-28(\cos\theta-\cos 3\theta)l(\theta)+32s_1(\theta)$$

$$-3(5-4\cos 2\theta-\cos 4\theta)\left(3l^2(\theta)-\frac{\pi^2}{4}\right)\Big\}\Big],$$

$$g_3^6=\frac{t^3}{\mu}\frac{2}{\pi^3}\Big[\Big\{8\cos\theta+4(1+\cos 2\theta)l(\theta)+2(\cos\theta-\cos 3\theta)\left(l^2(\theta)-\frac{\pi^2}{4}\right)$$

$$+(1-\cos 4\theta)\left(l^3(\theta)+\frac{\pi^2}{4}l(\theta)\right)\Big\}$$

$$\pm i\frac{\pi}{2}\Big\{4(1+\cos 2\theta)-4(\cos\theta-\cos 3\theta)l(\theta)-(1-\cos 4\theta)\left(l^2(\theta)+\frac{\pi^2}{4}\right)\Big\}\Big],$$

$$f_3^6=-\frac{t^3}{\mu}\frac{2}{\pi^3}\Big\{\left(\frac{8}{3}+\frac{2\pi^2}{9}\right)\cos\theta+\frac{2\pi^2}{3}\cos 3\theta+4(1+\cos 2\theta)l(\theta)$$

$$-2(\cos\theta-\cos 3\theta)\left(l^2(\theta)-\frac{\pi^2}{4}\right)-\frac{1}{3}(1-\cos 4\theta)\left(l^3(\theta)+\frac{\pi^2}{4}l(\theta)\right)\Big\}$$

$$-i\Im(g_3^6),$$

$$g_3^7=\overline{f_3^7},$$

$$f_3^7=\frac{t^3}{\mu}\frac{1}{6\pi^3}\Big[\Big\{56\cos\theta+20\pi^2(1-\cos\theta)-20(1-\cos 2\theta)l(\theta)$$

$$+22(\cos\theta-\cos 3\theta)\left(l^2(\theta)-\frac{\pi^2}{4}\right)$$

$$-80(s_2(\theta)+\sigma_2)+3(7-4\cos 2\theta-3\cos 4\theta)\left(l^3(\theta)-\frac{3\pi^2}{4}l(\theta)\right)\Big\}$$

$$\mp i\frac{\pi}{2}\Big\{20(1-\cos 2\theta)-44(\cos\theta-\cos 3\theta)l(\theta)+160s_1(\theta)$$

$$-3(7-4\cos 2\theta-3\cos 4\theta)\left(3l^2(\theta)-\frac{\pi^2}{4}\right)\Big\}\Big],$$

$$g_3^8=-\frac{t^3}{\mu}\frac{1}{\pi^3}\Big[\Big\{-\left(8+\frac{7\pi^2}{2}\right)\cos\theta-\frac{\pi^2}{2}\cos 3\theta+4(3+\cos 2\theta)l(\theta)$$

$$+2(3\cos\theta+5\cos 3\theta)l^2(\theta)+(1-4\cos 2\theta+3\cos 4\theta)\left(l^3(\theta)+\frac{\pi^2}{4}l(\theta)\right)\Big\}$$

$$\pm i\frac{\pi}{2}\Big\{4(1+3\cos 2\theta)+4(5\cos\theta+3\cos 3\theta)l(\theta)$$

$$+(1-4\cos 2\theta+3\cos 4\theta)\left(l^2(\theta)+\frac{\pi^2}{4}\right)\Big\}\Big],$$

$$f_3^8=\frac{t^3}{\mu}\frac{1}{\pi^3}\Big\{(8-2\pi^2)\cos\theta+2\pi^2\cos 3\theta+4(1+3\cos 2\theta)l(\theta)$$

$$+2(5\cos\theta+3\cos 3\theta)\left(l^2(\theta)-\frac{\pi^2}{4}\right)$$

$$+\frac{1}{3}(1-4\cos 2\theta+3\cos 4\theta)\left(l^3(\theta)+\frac{\pi^2}{4}l(\theta)\right)\Big\}-i\Im(g_3^8),$$

$$g_3^{10}=\frac{t^3}{\mu^3}\frac{4}{\pi^3}\Big[\Big\{\left(8-\frac{5\pi^2}{2}\right)\cos\theta+\frac{\pi^2}{2}\cos 3\theta+4(1+3\cos 2\theta)l(\theta)$$

$$+2(\cos\theta+3\cos 3\theta)l^2(\theta)-(1-\cos 4\theta)\left(l^3(\theta)+\frac{\pi^2}{4}l(\theta)\right)\Big\}$$

$$\pm i\frac{\pi}{2}\Big\{4(3+\cos 2\theta)+4(3\cos\theta+\cos 3\theta)l(\theta)$$

$$-(1-\cos 4\theta)\left(l^2(\theta)+\frac{\pi^2}{4}\right)\Big\}\Big],$$

$$f_3^{10}=-\frac{t^3}{\mu^3}\frac{4}{\pi^3}\Big\{\left(\frac{8}{3}+\frac{2\pi^2}{9}\right)\cos\theta+\frac{2\pi^2}{3}\cos 3\theta+4(3+\cos 2\theta)l(\theta)$$

$$+2(3\cos\theta+\cos 3\theta)\left(l^2(\theta)-\frac{\pi^2}{4}\right)$$

$$-\frac{1}{3}(1-\cos 4\theta)\left(l^3(\theta)+\frac{\pi^2}{4}l(\theta)\right)\Big\}-i\Im(g_3^{10}),$$

$$g_3^{11}=\frac{t^3}{\mu^3}\frac{8}{3\pi^3}\Big[\Big\{2\pi^2+\left(8-\frac{5\pi^2}{2}\right)\cos\theta+\frac{\pi^2}{2}\cos 3\theta-4(1-3\cos 2\theta)l(\theta)$$

$$+2\pi^2\cos\theta(1-\cos\theta)l(\theta)-4\pi^2\cos\theta\, s_1(\theta)-6(\cos\theta-\cos 3\theta)l^2(\theta)$$

$$-8(s_2(\theta)+\sigma_2)-(1-\cos 4\theta)\left(l^3(\theta)+\frac{\pi^2}{4}l(\theta)\right)-8\cos\theta(s_2(\theta)+\sigma_2)l(\theta)\Big\}$$

$$\pm i\frac{\pi}{2}\Big\{2\pi^2\cos\theta(1-\cos\theta)+4(3-\cos 2\theta)+4(\cos\theta-\cos 3\theta)l(\theta)+16s_1(\theta)$$

$$+(1-\cos 4\theta)\left(l^2(\theta)+\frac{\pi^2}{4}\right)+16\cos\theta\, s_1(\theta)l(\theta)-8\cos\theta(s_2(\theta)+\sigma_2)\Big\}\Big],$$

$$f_3^{11}=\frac{t^3}{\mu^3}\frac{8}{3\pi^3}\Big\{\frac{4\pi^2}{3}+16\sigma_2+\left(\frac{8}{3}+\frac{8\pi^2}{9}\right)\cos\theta+\frac{2\pi^2}{3}\cos 3\theta-\frac{2\pi^2}{3}\cos\theta(1-\cos\theta)$$

$$-4(3-\cos 2\theta)l(\theta)-2(\cos\theta-\cos 3\theta)\left(l^2(\theta)-\frac{\pi^2}{4}\right)-8(s_2(\theta)-\sigma_2)$$

$$-\frac{1}{3}(1-\cos 4\theta)\left(l^3(\theta)+\frac{\pi^2}{4}l(\theta)\right)-8\cos\theta(s_2(\theta)-\sigma_2)l(\theta)$$

$$+\frac{16}{3}\cos\theta(s_3(\theta)+\sigma_3)\Big\}-i\Im(g_3^{11}),$$

$$g_3^{12}=\overline{f_3^{12}},$$

$$f_3^{12}=\frac{t^3}{\mu^3}\frac{4}{\pi^3}\Big[\Big\{-8\cos\theta+12(1-\cos 2\theta)l(\theta)+6(\cos\theta-\cos 3\theta)\left(l^2(\theta)-\frac{\pi^2}{4}\right)$$

$$+(5-4\cos 2\theta-\cos 4\theta)\left(l^3(\theta)-\frac{3\pi^2}{4}l(\theta)\right)\Big\}$$

$$\pm i\frac{\pi}{2}\Big\{12(1-\cos 2\theta)+12(\cos\theta-\cos 3\theta)l(\theta)$$

$$+(5-4\cos 2\theta-\cos 4\theta)\left(3l^2(\theta)-\frac{\pi^2}{4}\right)\Big\}\Big],$$

$$g_3^{19}+g_3^{22}=\frac{t^3}{\mu^3}\frac{4}{\pi^3}\Big[\Big\{(8+\pi^2)\cos\theta+\pi^2\cos 3\theta-4(1-3\cos 2\theta)l(\theta)$$

$$-6(\cos\theta-\cos 3\theta)l^2(\theta)-(1-\cos 4\theta)\left(l^3(\theta)+\frac{\pi^2}{4}l(\theta)\right)\Big\}$$

$$\pm i\frac{\pi}{2}\Big\{4(1+\cos 2\theta)-4(\cos\theta-\cos 3\theta)l(\theta)-(1-\cos 4\theta)\left(l^2(\theta)+\frac{\pi^2}{4}\right)\Big\}\Big],$$

$$f_3^{19}+f_3^{22}=-\frac{t^3}{\mu^3}\frac{4}{\pi^3}\Big\{\left(\frac{8}{3}+\frac{2\pi^2}{9}\right)\cos\theta+\frac{2\pi^2}{3}\cos 3\theta+4(1+\cos 2\theta)l(\theta)$$

$$-2(\cos\theta-\cos 3\theta)\left(l^2(\theta)-\frac{\pi^2}{4}\right)-\frac{1}{3}(1-\cos 4\theta)\left(l^3(\theta)+\frac{\pi^2}{4}l(\theta)\right)\Big\}$$

$$-i\Im(g_3^{19}+g_3^{22}),$$

$$g_3^{20}+2g_3^{23}=\frac{t^3}{\mu^3}\frac{4}{\pi^3}\Big[\Big\{\left(8-\frac{5\pi^2}{2}\right)\cos\theta+\frac{\pi^2}{2}\cos 3\theta-12(1-\cos 2\theta)l(\theta)$$

$$-6(\cos\theta-\cos 3\theta)l^2(\theta)-8(s_2(\theta)+\sigma_2)-(1-\cos 4\theta)\left(l^3(\theta)+\frac{\pi^2}{4}l(\theta)\right)\Big\}$$

$$\pm i\frac{\pi}{2}\Big\{4(1-\cos 2\theta)+4(\cos\theta-\cos 3\theta)l(\theta)+16s_1(\theta)$$

$$+(1-\cos 4\theta)\Big(l^2(\theta)+\frac{\pi^2}{4}\Big)\Big\}\Big],$$

$$f_3^{20}+2f_3^{23}=\frac{t^3}{\mu^3}\frac{4}{\pi^3}\Big\{\Big(\frac{8}{3}-\frac{16\pi^2}{9}\Big)\cos\theta+\frac{2\pi^2}{3}\cos 3\theta-4(1-\cos 2\theta)l(\theta)$$

$$-2(\cos\theta-\cos 3\theta)\Big(l^2(\theta)-\frac{\pi^2}{4}\Big)-8(s_2(\theta)+\sigma_2)$$

$$-\frac{1}{3}(1-\cos 4\theta)\Big(l^3(\theta)+\frac{\pi^2}{4}l(\theta)\Big)\Big\}-i\Im(g_3^{20}+2g_3^{23}),$$

$$g_3^{21}+2g_3^{24}=\frac{t^3}{\mu^3}\frac{2}{\pi^3}\Big[\Big\{8\frac{\cos\theta}{\sin^2\theta}+8\cos\theta-4(1-3\cos 2\theta)l(\theta)$$

$$-6(\cos\theta-\cos 3\theta)\Big(l^2(\theta)+\frac{\pi^2}{12}\Big)+(3-4\cos 2\theta+\cos 4\theta)\Big(l^3(\theta)+\frac{\pi^2}{4}l(\theta)\Big)\Big\}$$

$$\pm i\frac{\pi}{2}\Big\{4(3-\cos 2\theta)+4(\cos\theta-\cos 3\theta)l(\theta)$$

$$-(3-4\cos 2\theta+\cos 4\theta)\Big(l^2(\theta)+\frac{\pi^2}{4}\Big)\Big\}\Big],$$

$$f_3^{21}+2f_3^{24}=\frac{t^3}{\mu^3}\frac{2}{\pi^3}\Big\{-8\frac{\cos\theta}{\sin^2\theta}+\Big(\frac{8}{3}-\frac{22\pi^2}{9}\Big)\cos\theta+\frac{2\pi^2}{3}\cos 3\theta$$

$$-4(3-\cos 2\theta)l(\theta)-2(\cos\theta-\cos 3\theta)\Big(l^2(\theta)-\frac{\pi^2}{4}\Big)$$

$$+\frac{1}{3}(3-4\cos 2\theta+\cos 4\theta)\Big(l^3(\theta)+\frac{\pi^2}{4}l(\theta)\Big)\Big\}-i\Im(g_3^{21}+2g_3^{24}).$$

The expressions for pairs $g_3^2+f_3^2$, $g_3^5+f_3^5$, $g_3^9+f_3^9$, and $g_3^{13}+f_3^{13}\sim g_3^{18}+f_3^{18}$ are omitted, since they do not contribute to the value of G_3 on the surface of the profile.

σ_2 and σ_3 are the constants defined in Appendix A.

The function G_3 is the linear combination of g_3^j and f_3^j:

$$G_3=f_3^0+\sum_{j=1}^{24}B^j(g_3^j+f_3^j),$$

where B^j are coefficients determined by M, γ and ν as given in I–(3.8). The third approximation of the velocity potential, ϕ_3, is the real part of G_3.

C. The Incompressible Flow past a Symmetrical Circular Arc Aerofoil

As is well known, the region outside a symmetrical circular arc aerofoil in the z-plane (see Fig. 1) is mapped onto the region outside the unit circle in the Z-plane by the following transformation due to von Kármán and Trefftz:

$$\frac{z-1}{z+1}=\left(\frac{Z-1}{Z+1}\right)^{\kappa}, \qquad \kappa=2-\frac{4\beta}{\pi}. \tag{C.1}$$

Here is designated the chord length of the aerofoil as 2, and the velocity of the undisturbed flow as unity. Since $\lim_{Z\to\infty}\frac{dz}{dZ}=1/\kappa$, the velocity potential Φ is determined as follows:

$$\Phi=\frac{1}{\kappa}\left(Z+\frac{1}{Z}\right). \tag{C.2}$$

At the surface of the profile ($Z=e^{i\theta}$),

$$\Phi=\frac{2}{\kappa}\cos\theta, \qquad \frac{d\Phi}{d\theta}=-\frac{2}{\kappa}\sin\theta, \tag{C.3}$$

$$z=\frac{1+\left(i\tan\frac{\theta}{2}\right)^{\kappa}}{1-\left(i\tan\frac{\theta}{2}\right)^{\kappa}}=\frac{2\left\{1-\left(\tan\frac{\theta}{2}\right)^{\kappa}\cos\frac{\kappa\pi}{2}\right\}-i2\left(\tan\frac{\theta}{2}\right)^{\kappa}\sin\frac{\kappa\pi}{2}}{1-2\left(\tan\frac{\theta}{2}\right)^{\kappa}\cos\frac{\kappa\pi}{2}+\left(\tan\frac{\theta}{2}\right)^{2\kappa}}-1, \tag{C.4}$$

$$\frac{d\theta}{ds}=\mp\left|\frac{d\theta}{dz}\right|=\mp\frac{\sin\theta}{2\kappa}\left\{\left(\tan\frac{\theta}{2}\right)^{\kappa}+\left(\tan\frac{\theta}{2}\right)^{-\kappa}-2\cos\frac{\kappa\pi}{2}\right\}. \tag{C.5}$$

Then the magnitude of the velocity at the surface is given by the formula:

$$q=\frac{d\Phi}{d\theta}\frac{d\theta}{ds}=\frac{\sin^2\theta}{\kappa^2}\left\{\left(\tan\frac{\theta}{2}\right)^{\kappa}+\left(\tan\frac{\theta}{2}\right)^{-\kappa}-2\cos\frac{\kappa\pi}{2}\right\}. \tag{C.6}$$

If the thickness ratio $t=\tan^{-1}\beta$ is sufficiently small, those terms containing κ can be expanded into series in β, especially

$$\left(\tan\frac{\theta}{2}\right)^{\kappa}=\left(\tan\frac{\theta}{2}\right)^{2}\left\{1-\frac{4\beta}{\pi}l(\theta)+\frac{8\beta^2}{\pi^2}l^2(\theta)-\frac{32\beta^3}{3\pi^3}l^3(\theta)+\cdots\cdots\right\},$$

where

$$l(\theta)=\log\left|\tan\frac{\theta}{2}\right|.$$

Accordingly we can obtain the expansion formulae in β for $x(\theta)$, $y(\theta)$, $\Phi(\theta)$ and $q(\theta)$. By changing parameter from β to t, we can easily verify that these formulae are in perfect accord with the expressions obtained in §§ 3, 4 and 5, when $M=0$, as it ought to be.

In Table II, the results by the thin-wing-expansion method are compared with the exact solutions (C.4) and (C.6). The accuracy of the approximation is very good. Moreover even the second approximation seems to give satisfactory result, so long as the thickness ratio is less than about 0.1.

Table II. Velocity Distribution over the Surface of a Symmetrical Circular Arc Aerofoil, $t=0.1$; Incompressible Flow.

θ (deg.)	$x^{(1)}$	$x^{(2)}$	$x^{(3)}$	x (exact)	$q^{(1)}$	$q^{(2)}$	$q^{(3)}$	q (exact)
9	0.9837	0.9833	0.9833	0.9833	0.8076	0.8306	0.8293_5	0.8293_2
18	0.9399	0.9395	0.9394	0.9397	0.9042	0.9132	0.9129_9	0.9129_6
27	0.8723	0.8726	0.8724	0.8729	0.9655	0.9697	0.9696_6	0.9696_3
36	0.7843	0.7857	0.7854	0.7859	1.0115	1.0140	1.0137_9	1.0137_7
45	0.6791	0.6815	0.6813	0.6817	1.0480	1.0498	1.0494_5	1.0494_4
54	0.5597	0.5628	0.5627	0.5629	1.0769	1.0785	1.0781_1	1.0781_0
63	0.4292	0.4325	0.4325	0.4325	1.0990	1.1008	1.1002_8	1.1002_7
72	0.2906	0.2933	0.2934	0.2932	1.1148	1.1167	1.1161_2	1.1161_0
81	0.1466	0.1482	0.1482	0.1481	1.1242	1.1263	1.1256_4	1.1256_3
90	0	0	0	0	1.1273	1.1295	1.1288_2	1.1288_0

(1).....1st approx. (2).....2nd approx. (3).....3rd approx.

References

(1) Asaka, S. Nat. Sci. Rep. Ochanomizu Univ. **4** (1953) 213.
(2) Hasimoto, H. J. Phys. Soc. Jap. **7** (1952) 322.

(Received June 16, 1954)